

Decay of  $Mg^{27}$ 

W. S. LYON AND N. H. LAZAR  
*Oak Ridge National Laboratory, Oak Ridge, Tennessee*  
 (Received October 26, 1955)

The gamma rays accompanying the decay of 9.45-min  $Mg^{27}$  have been studied by use of a NaI scintillation spectrometer and beta-gamma coincidence counting. Three gamma rays of energies 0.834, 1.015, and 0.175 Mev were found with relative intensities of 1.00, 0.43, and 0.009. The isotopic thermal-neutron activation cross section for production of  $Mg^{27}$  is found to be  $25 \pm 2$  millibarns.

## INTRODUCTION

UNCERTAINTY exists in the literature as to the gamma-ray branching in  $Mg^{27}$ . Benes, Hedgran, and Hole<sup>1</sup> proposed a decay scheme in which the 1.01-Mev and 0.84-Mev gamma rays were in coincidence, with 20% of the decay through the 1.01-Mev gamma ray and 100% through the 0.84-Mev gamma ray. Daniel, Koester, and Mayer-Kuckuk<sup>2</sup> and Daniel and Bothe<sup>3</sup> reported the gamma rays to be not in coincidence with intensities of 42% for the 1.015-Mev gamma ray and 58% for the 0.84-Mev gamma ray. These observations were confirmed in part by Koester.<sup>4</sup> Only one reported value for the thermal-neutron activation cross section has been given. This is the value

of Seren *et al.*<sup>5</sup> of 50 millibarns. It thus seemed of interest to attempt clarification of the decay scheme of  $Mg^{27}$  and to redetermine the activation cross section.

## EXPERIMENTAL

Magnesium oxide (cp) was irradiated in the ORNL graphite reactor together with weighed amounts of manganese monitor metal for ten minutes. The  $MgO$  was dissolved in  $HNO_3$ , the solution made to volume and known aliquots taken for examination by use of the 3 in.  $\times$  3 in. NaI(Tl) gamma-ray spectrometer. In addition, aliquots were evaporated to dryness and used as sources for beta-gamma coincidence measurements. Decay measurements indicated the presence of  $\sim 1\%$  of the longer lived contaminants  $Mn^{56}$  and  $Na^{24}$ ; however, the disintegration rate determinations described below were made before the  $Mg^{27}$  had decayed to the extent that the contamination would create an

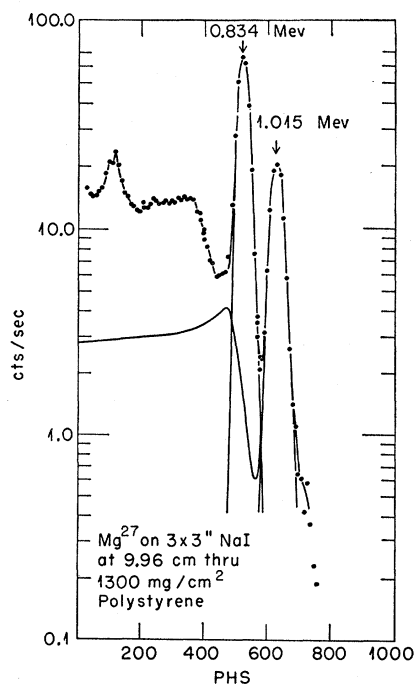


FIG. 1. Gamma-ray spectrum of  $Mg^{27}$  with no antineutron scatter collimator.

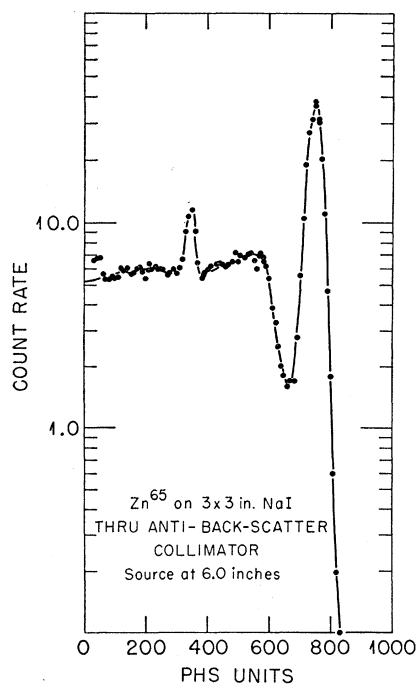


FIG. 2. Gamma-ray spectrum of  $Zn^{65}$  thru antineutron scatter collimator.

<sup>1</sup> Benes, Hedgran, and Hole, *Arkiv. Mat., Astron. Fysik* **35A** No. 12 (1948).

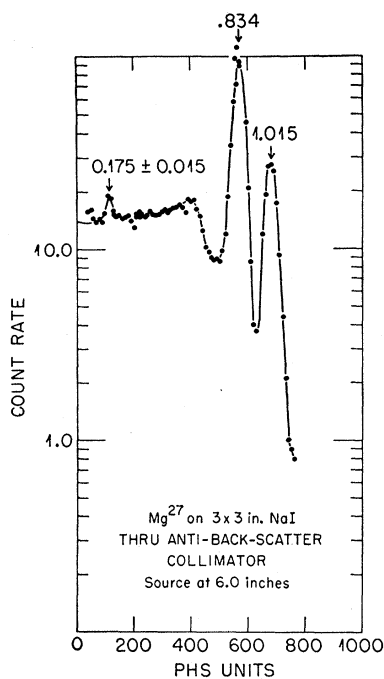
<sup>2</sup> Daniel, Koester, and Mayer-Kuckuk, *Z. Naturforsch.* **8A**, 447 (1953).

<sup>3</sup> H. Daniel and W. Bothe, *Z. Naturforsch.* **9A**, 402 (1954).

<sup>4</sup> L. Koester, *Z. Naturforsch.* **9A**, 104 (1954).

<sup>5</sup> Seren, Friedlander, and Turkel, *Phys. Rev.* **72**, 888 (1947).

Fig. 3. Gamma-ray spectrum of  $Mg^{27}$  thru antibackscatter collimator.



error of more than a few percent. The evaporated aliquots for coincidence counting were placed between the beta detector (A- $CH_4$   $\beta$  proportional counter) and the gamma detector (NaI gamma-ray spectrometer set on the 0.834-Mev gamma-ray photopeak). The disintegration rate as a function of aluminum absorber before the beta detector was obtained and found to be constant over the range 0–49 mg/cm<sup>2</sup>.

The  $Mn^{56}$  activity induced in the Mn monitor metal was measured by use of a calibrated high-pressure ion chamber, and the average neutron flux calculated. By use of this flux, the thermal-neutron cross section for production of  $Mn^{56}$  (13.4 barns<sup>6</sup>) and the specific activity of the  $Mg^{27}$  produced, the thermal-neutron cross section for production of  $Mg^{27}$  was calculated. (The specific activity of the  $Mg^{27}$  was found by dividing the disintegration rate of the  $Mg^{27}$  solution, determined from a  $\beta$ - $\gamma$  coincidence measurement, by the amount of magnesium present found by flame photometric analysis.) The isotopic cross section obtained was  $25 \pm 2$  millibarns.

Sources used for the gamma-ray spectrum study were put through a chemical separation to remove contaminants. This procedure consisted of three  $Fe(OH)_3$  precipitations from ammoniacal solution to remove  $Mn^{56}$ , followed by precipitation of  $Mg(OH)_2$  from NaOH solution. The  $Mg(OH)_2$  was washed with dilute NaOH to remove  $Na^{24}$ , the  $Mg(OH)_2$  dissolved in  $HNO_3$ , and  $Mg(OH)_2$  reprecipitated by addition

<sup>6</sup> D. J. Hughes and J. A. Harvey, *Neutron Cross Sections*, Brookhaven National Laboratory Report BNL-325 (Superintendent of Documents, U. S. Government Printing Office, Washington, D. C., 1955).

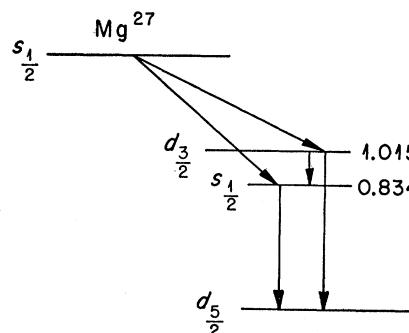


Fig. 4. Decay scheme of  $Mg^{27}$ .

of more NaOH. Three separate precipitations were made. The final precipitate was used as a source on a 3 in.  $\times$  3 in. NaI gamma-ray spectrometer used in conjunction with a twenty-channel analyzer.

### RESULTS AND DISCUSSION

Figure 1 shows the pulse-height spectrum obtained from a source of  $Mg^{27}$  placed 9.3 cm from the cylindrical 3 in.  $\times$  3 in. NaI spectrometer. The relative intensities of the two gamma rays at 1.015 and 0.834 Mev were determined from their measured peak areas,  $P(\gamma)$ , and the expression

$$I(\gamma) = P(\gamma) / \epsilon_p \Omega,$$

where  $\epsilon_p$  is the experimentally determined peak efficiency for the particular crystal and geometry, and  $\Omega$  is the fraction of the total solid angle subtended by the crystal at the source. The ratio,

$$I(\gamma) / [I(0.834) + I(1.015)],$$

for the 0.834- and 1.015-Mev  $\gamma$  rays, is  $0.70 \pm 0.05$  and  $0.30 \pm 0.02$ , respectively. The Compton edge from the 1.015-Mev  $\gamma$  ray was subtracted from under the 0.834-Mev peak, using the shape of the spectrum obtained from the 1.114-Mev  $\gamma$  ray in  $Zn^{65}$  under the same experimental conditions.

As mentioned in the introduction, these two gamma rays have been found not to be in coincidence so the cascade gamma ray of  $\sim 180$  kev expected to occur between the two states was looked for. Because of the large peak found in the spectrum in this region (Fig. 1) due to Compton scattering of  $\gamma$  rays from the walls of the lead shield used to reduce general room background, whether or not such a  $\gamma$  ray exists could not be directly determined. To remove this back-scatter peak, the source was placed at the apex of a conical hole cut into a table made of 2-in. lead bricks. The crystal was placed under the table in the lead shield so that it could see into the surroundings of the source only through the conical collimator. The pulse height spectrum obtained in this way for a source of  $Zn^{65}$  is shown in Fig. 2. A run obtained with a  $Mg^{27}$  sample is shown in Fig. 3. The intensity of the gamma ray at  $0.175 \pm 0.015$  Mev is 2.2% of the 1.015-Mev  $\gamma$  ray.

During the coincidence measurements for the cross-section determination, a measured aliquot of the  $\text{Mg}(\text{OH})_2$  was used to yield the absolute intensity of the gamma rays. This was determined from a measurement of the 1.015-Mev peak area and the ratio of the  $\gamma$  rays previously determined. The disintegration rate of the source was compared to the total gamma ray intensity and found to agree within 5%, thus corroborating the lack of coincidences between the two gamma rays. From this measurement, one can state all  $\beta$ -ray transitions occur to the excited states within this experimental uncertainty.

The decay scheme shown in Fig. 4 may now be constructed. The spin assigned to  $\text{Mg}^{27}$  is  $s_{\frac{1}{2}}$  on the basis of single-particle considerations and the lack of  $\beta$

transitions to the measured  $5/2$  spin ground state of  $\text{Al}^{27}$ .<sup>7</sup> The assignments for the excited states of  $\text{Al}^{27}$  are in agreement with the beta-ray observations, but are based primarily on single particle considerations and the relative intensities of the  $\gamma$  rays. The shell model states predicted, in this region, for the 13th proton are  $d_{\frac{3}{2}}$ ,  $d_{\frac{5}{2}}$ , and  $s_{\frac{1}{2}}$  (not necessarily in this order), and the possible order of the spins of the excited states is still open to question. The probability for the 0.175-Mev transition relative to the cross-over  $\gamma$  ray computed from the indicated spins and the Weisskoff formula is  $\sim 1\%$  in agreement with the observed intensity of 2.2%. This transition would be expected to be considerably more intense if the spins were reversed.

<sup>7</sup>J. E. Mack, *Revs. Modern Phys.* **22**, 64 (1950).

## Disintegration of Hyperfragments. II\*

W. F. FRY, J. SCHNEPS, AND M. S. SWAMI

*Department of Physics, University of Wisconsin, Madison, Wisconsin*

(Received November 28, 1955)

The systematic study of hyperfragments has been continued. A total of 32 000 cosmic-ray stars, 10 000 6-Bev proton stars, 32 000 3-Bev  $\pi^-$ -meson stars and 206 stars produced by stopped negative  $K$  mesons were examined. Twenty hyperfragments were found in the cosmic-ray plates, 7 in the proton plates, 30 in the  $\pi^-$ -meson plates and 11 in the negative  $K$ -meson plates. The average charge of the hyperfragments is between 4 and 5. The average range of the hyperfragments is about 10 microns. Including previous data from this laboratory, only 2 mesonic decays have been found out of 98 events with  $Z$  greater than 2. A total of 7 helium hyperfragments have been observed of which 4 decayed mesonically. Of 4 hydrogen hyperfragments, all decayed with the emission of a  $\pi^-$  meson. In the following eight cases, it was possible to measure the total energy release in the hyperfragment disintegration, and hence to find the following values (in Mev) for the binding energy of the  $\Lambda^0$  particle:  ${}_{\Lambda}\text{H}^3(B_{\Lambda}=0.6\pm 0.6)$ ;  ${}_{\Lambda}\text{H}^3(B_{\Lambda}=-0.5\pm 0.6)$ ;  ${}_{\Lambda}\text{H}^3(B_{\Lambda}=0.4\pm 0.7)$ ;  ${}_{\Lambda}\text{H}^4(B_{\Lambda}=0.5\pm 2.0$  or  $1.9\pm 2.0)$ ;  ${}_{\Lambda}\text{He}^4(B_{\Lambda}=0.0\pm 2.0)$ ;  ${}_{\Lambda}\text{He}^4(B_{\Lambda}=1.8\pm 0.6)$

${}_{\Lambda}\text{He}^5(B_{\Lambda}=2.0\pm 0.6)$ ;  ${}_{\Lambda}\text{Be}^9(B_{\Lambda}=6.5\pm 0.6)$ . The binding energies tend to increase with increasing mass number. The fact that  ${}_{\Lambda}\text{H}^4$  and  ${}_{\Lambda}\text{He}^5$  hyperfragments exist, plus the fact that the binding energy of the  $\Lambda^0$  particle in  ${}_{\Lambda}\text{Be}^9$  is greater than that of the last neutron in  $\text{Be}^9$ , shows that the Pauli principle need not be considered for a  $\Lambda^0$  particle bound in a nucleus. If the binding of the  $\Lambda^0$  particle can be described in terms of a potential well the depth of the well is greater than 6.5 Mev, as indicated by  $B_{\Lambda}$  for  ${}_{\Lambda}\text{Be}^9$ . In light hyperfragments the low binding energies imply that the  $\Lambda^0$  particle spends much of its time outside the nucleus. The momentum of the  $\Lambda^0$  particle has been measured in several light hyperfragments where a  $\pi^-$  meson and proton were emitted, by assuming it to be equal to the momentum of the  $\pi^-$  meson and proton. In general the momentum values are quite low, which supports the hypothesis that the bound  $\Lambda^0$  particle spends considerable time outside the nucleus. No further examples of energetic hyperfragments, as have been previously reported, were found in this work.

### INTRODUCTION

FOLLOWING the discovery by Danysz and Pniewski<sup>1</sup> of the decay of a hyperfragment, many cases have been observed where the binding energy of the  $\Lambda^0$  hyperon could be evaluated.

The program for the systematic study of the production and decay of hyperfragments, some of the results of which have been reported in a previous paper,<sup>2</sup> has been continued. Additional hyperfragments produced by cosmic rays, high-energy protons,  $\pi^-$  mesons, and stopped  $K^-$ -mesons are reported in this paper.

\* Supported in part by the U. S. Atomic Energy Commission and by the Graduate School from funds supplied by the Wisconsin Alumni Research Foundation.

<sup>1</sup>M. Danysz and J. Pniewski, *Phil. Mag.* **44**, 348 (1953).

<sup>2</sup>Fry, Schneps, and Swami, *Phys. Rev.* **99**, 1561 (1955). This paper will be referred to as I.

### PROCEDURE

Stacks of 600 micron pellicles were exposed to 6-Bev protons, 3-Bev  $\pi^-$  mesons, and stopped  $K^-$ -mesons<sup>3</sup> from the Berkeley Bevatron. Additional stacks were exposed to cosmic rays in a skyhook balloon flight. These pellicles were area scanned for stars with a low magnification. The identification and selection criteria for hyperfragments were essentially the same as in the previous work (I).

### OBSERVATIONS

#### A. General Features

The frequencies of hyperfragments from the various exposures are given in Table I. In many of the events

<sup>3</sup>Fry, Schneps, Snow, and Swami, *Phys. Rev.* **100**, 1448 (1955); **100**, 950 (1955).